Available online at www.sciencedirect.com
ScienceDirect
Journal of Molecular Catalysis A: Chemical 280 (2008) 203–209
JOURNAL OF MOLECULAR CATALYSIS A: CHEMICAL
www.elsevier.com/locate/molcata

Catalase mimics of a manganese(II) complex: The effect of axial ligands and pH

József Kaizer [a], Tamás Csay [a], Péter Kővári [a], Gábor Speier [a,*], László Párkányi [b]

[a] *Department of Chemistry, University of Pannonia, H-8200 Veszprém, Hungary*
[b] *Chemical Research Center, Institute of Structural Research, Hungarian Academy of Sciences, P.O. Box 17, H-1525 Budapest, Hungary*

Received 23 August 2007; received in revised form 5 November 2007; accepted 6 November 2007
Available online 13 November 2007

Abstract

The mononuclear $[Mn(indH)Cl_2](CH_3OH)$ (indH: 1,3-bis(2′-pyridylimino)-isoindoline) complex has been prepared and characterized by various techniques such as elemental analysis, IR, UV–vis, ESR spectroscopy and X-ray diffraction. The title compound in the presence of a base such as 1-methylimidazole, imidazole or pyridine is efficient catalyst for the disproportionation of H_2O_2 in CH_3CN. Among the various nitrogenous bases investigated in this study imidazole and substituted imidazoles with strong π-donating ability show better co-catalytic effect.

In case of aqueous solution the complex $[Mn(indH)Cl_2](CH_3OH)$ shows much higher catalytic activity, and the initial rate of the disproportionation of H_2O_2 increases with increasing pH and goes through a maximum, which was found at pH ∼ 9.6. In this pH value the reaction shows first-order dependence on the catalyst, and saturation kinetics on $[H_2O_2]$ with $V_{max} = 8.1 \times 10^{-3}\ Ms^{-1}$, $K_M = 489$ mM, $k_{cat} = 38 \pm 2\ s^{-1}$ and $k_2(k_{cat}/K_M) = 79 \pm 4\ M^{-1}s^{-1}$.

Keywords: Biomimetic oxidation; Hydrogen peroxide; Catalase activity; Kinetic studies; Manganese(II)

1. Introduction

Catalases are enzymes that disproportionate hydrogen peroxide into H_2O and O_2, and thereby protect living organisms from reactive oxygen species (ROS) that are responsible for "oxidative stress" reactions in the cell leading *e.g.* to aging [1,2]. Besides heme type catalases, there is a class of manganese catalases which has been isolated from several bacterial organisms: *Lactobacillus plantarum* [3,4], *Thermus thermophilus* [5], *Thermoleophilium album* [6], *Thermus* sp. YS 8–13 [7], and *Pyrobaculum calidifontis* VA1 [8]. The structural aspects of catalysis are of great current interest for these enzymes; furthermore synthetic catalytic scavengers of ROS would be clinically superior to stoichiometric ones [9–11]. Among them, salen–manganese complexes seem promising, because they exhibit dual functions, *i.e.* superoxide dismutase- and catalase-mimetic activities [12,13]. 1,3-Bis(2′-pyridylimino)isoindoles, which have recently received increased attention, are restricted to coordinate in a meridional fashion about the metal center, thus imparting trigonal symmetry on pentacoordinate metal ions. Ruthenium [14], cobalt [15], copper [16], and iron [17] complexes of 1,3-bis(2′-pyridylimino)isoindoline were used as catalyst in various oxidation and oxygenation reactions. Our approach was to design a highly active manganese(II) complex of the 1,3-bis(2′-pyridylimino)isoindoline (indH) ligand and increase its catalase-like activity by introducing various nitrogen-containing ligands such as imidazole, since its presence in many biological systems provides a potential binding site for metal ions.

2. Experimental

2.1. Materials

All manipulations were performed under a pure dinitrogen or argon atmosphere unless otherwise stated, using standard Schlenck-type inert-gas techniques [18]. Solvents used for the reactions were purified by literature methods [19] and stored

* Corresponding author.
E-mail address: speier@almos.vein.hu (G. Speier).

1381-1169/$ – see front matter © 2007 Elsevier B.V. All rights reserved.
doi:10.1016/j.molcata.2007.11.005

under argon. 1,3-Bis′(2-pyridylimino)isoindoline (indH) was prepared according to the literature [20]. All other chemicals were commercial products and were used as received without further purification.

2.2. Analytical and physical measurements

Infrared spectra were recorded on an Avatar 330 FT-IR Thermo Nicolet instrument using samples mulled in Nujol between KBr plates or in KBr pellets. UV–vis spectra were recorded on a Shimadzu UV-160 spectrophotometer using quartz cells. Electron spin resonance (ESR) spectra were recorded in a Bruker ELEXYS E500 CW EPR in dmf solution. Microanalyses were done by the Microanalytical Service of the University. Single crystals of $[Mn(indH)Cl_2](CH_3OH)$ suitable for an X-ray diffraction study were grown from ethanol by ether diffusion. The intensity data were collected with Rigaku R-AXIS Rapid single-crystal diffractometer using Mo Kα radiation (λ = 0.71070 Å) at 293 K. Crystallographic data and details of the structure determination are given in Table 1, whereas selected bond lengths and angles are listed in Table 2. SHELX-97 [21] was used for structure solution and full matrix least squares refinement on F^2. The SUEEZE function of PLATON was used to eliminate the contribution from the heavily disordered methanol solvent. Crystal structure has been deposited at the Cambridge Crystallographic Data Centre (Deposition no. CCDC 639410).

Table 1
Summary of the crystallographic data and structure parameters for $[Mn(indH)Cl_2](CH_3OH)$

Formula weight	425.17
Crystal system	Monoclinic
Crystal description	Block
Space group	*C*2/*c*
Unit cell dimensions	
a (Å)	15.052 (10)
b (Å)	15.964 (8)
c (Å)	15.870 (11)
α (°)	90.00
β (°)	90.66 (2)
γ (°)	90.00
Volume (Å^3)	3813 (4)
Z	8
Calculated density (g cm^{-1})	1.481
Crystal size (mm^3)	0.45 × 0.36 × 0.23
Index ranges	$-17 \le h \le 17$
	$-18 \le k \le 18$
	$-18 \le l \le 18$
Temperature (K)	293 (2)
Radiation	Mo Kα (λ = 0.71070)
Absorption coefficient (mm^{-1})	0.984
F(0 0 0)	1720
Reflections collected	3299
Observed reflections	1936
[$I > 2\sigma(I)$]	
Goodness-of-fit	1.295
Final *R* indices	$R_1 = 0.0632$, w$R_2 = 0.1469$
R indices (all data)	$R_1 = 0.1141$, w$R_2 = 0.1760$

Table 2
Selected bond lengths (Å) and bond angles (°) for $[Mn(indH)Cl_2](CH_3OH)$

Mn(1)–N(1)	2.152(4)	Mn(1)–Cl(1)	2.4063(19)
Mn1(1)–N(5)	2.236(5)	N(3)–C(4)	1.284(7)
Mn(1)–N(4)	2.261(5)	C(1)–N(2)	1.323(7)
Mn(1)–Cl(2)	2.373(2)		
N(5)–Mn(1)–N(4)	165.72(18)	Cl(1)–Mn(1)–Cl(2)	111.68(7)
N(1)–Mn(1)–Cl(1)	123.63(13)	C(4)–N(3)–C(14)	128.2(5)
N(1)–Mn(15)–Cl(2)	124.53(13)	C(1)–N(2)–C(9)	112.5(5)

2.3. Synthesis of $[Mn(indH)Cl_2](CH_3OH)$

A solution of 0.59 g (3 mmol) of $MnCl_2{\cdot}4H_2O$ in 10 cm^3 CH_3OH was added to a solution of 0.90 g (3 mmol) indH in 10 cm^3 CH_3CN and the yellow suspension was refluxed for 24 h. The solvent was removed by evaporation and the crude product was washed with cold CH_3OH and diethylether, and then dried under vacuum. The crude product was recrystallized from CH_3OH by ether diffusion. Yield: 0.89 g (65%). UV–vis (λ_{max}, dmf): 271 nm (*ε*, 15 488), 284 (19 953), 296 (19 953), 330 (17 378), 346 (17 782), 367 (19 055), 386 (21 878). IR (KBr): 3468, 3288, 3064, 2966, 2921, 1659, 1628, 1592, 1557, 1519, 1488, 1468, 1429, 1372, 1299, 1266, 1201, 1099, 1058, 866, 780, 711, 514, 416 cm^{-1}. ESR (dmf): $g = 2.0011$, $A = 94.14$ G. Anal. Calcd. for $C_{19}H_{17}ON_5MnCl_2$: C, 49.91; H, 3.75; N, 15.32; Cl, 15.51; Mn, 12.02. Found: C, 50.22; H, 3.84; N, 14.85; Cl, 15.14; Mn, 11.89%.

2.4. Catalase-like activity

All reactions were carried out at 21 °C in a 30 cm^3 reactor containing a stirring bar under air. In a typical experiment CH_3CN (20 cm^3) or the appropriate aqueous solution (20 cm^3 carbonate: 0.1 M, pH 10.23, 10.36, 10.56; or ammonium hydroxide: 0.2 M: 9.16, 9.52, 9.72 buffer) was added to the complex and the flask was closed with a rubber septum. Hydrogen peroxide was injected through the septum with a syringe. The reactor was connected to a graduated burette filled with oil and dioxygen evolution was measured volumetrically at time intervals of ∼20 s. Observed initial rates were expressed as Ms^{-1} by taking the volume of the solution into account and calculated from the maximum slope of curve describing evolution of O_2 *versus* time.

3. Results and discussion

3.1. Synthesis and characterization of the $[Mn(indH)Cl_2](CH_3OH)$

Reaction of equimolar amounts of 1,3-bis(2′-pyridylimino)isoindoline and $MnCl_2{\cdot}4H_2O$ in methanol resulted in the formation of $[Mn(indH)Cl_2](CH_3OH)$. The Mn(II) ion is bound to a neutral tridentate isoindoline ligand and two chloride anions, forming a distorted trigonal bipyramidal environment around the metal ion. Analytical data, the infrared and the electronic spectrum of the complex are all consistent with the presence of a neutral nondeprotonated isoindoline ligand.

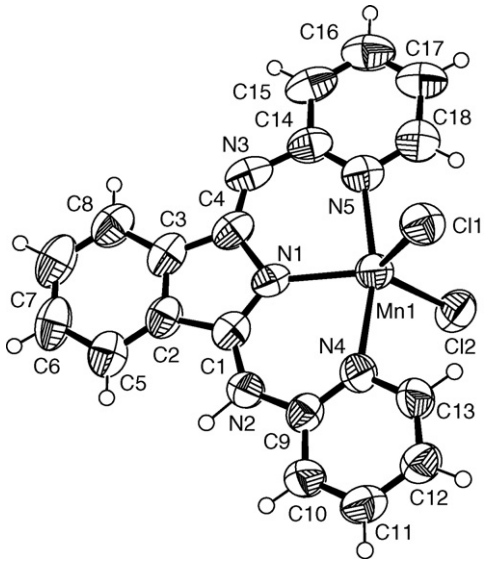

Fig. 1. Ellipsoid drawing of $[Mn(indH)Cl_2](CH_3OH)$ with the atom numbering scheme.

Infrared spectra of metal complexes with deprotonated ligand *versus* nondeprotonated ligand show substantial differences in the region 1450–1660 cm^{-1} [22]. The infrared spectrum of $[Mn(indH)Cl_2](CH_3OH)$ has two strong absorptions at 1659 and 1628 cm^{-1}, and one weak at 3288 cm^{-1}, characteristic of a coordinated nondeprotonated isoindoline ligand. Complexes that contain deprotonated isoindoline ligands only exhibit weak bands above 1600 cm^{-1} [23,24]. These absorptions cannot be readily assigned to a specific vibration but may be coupled modes involving the imines and the 2-pyridine groups. A broad band in the region around 3470 cm^{-1} indicates the presence of ν(OH) of methanol molecules for the title compound. The peak around 2900 cm^{-1} [$\nu(CH_{aliph})$] can be assigned to the coordinated CH_3OH. The electronic spectrum of the [Mn(indH)Cl_2](CH_3OH) complex is dominated by the π–π^* transitions of the neutral ligand indH. Deprotonation of the pyrrole nitrogen could be reduced the difference in energy between occupied and unoccupied π-MOs of the ligand and resulted in a red shift of π–π^* transitions (50–100 nm) [24]. The ESR spectra also provide information upon the nature of Mn species present. The solution spectra of [Mn(indH)Cl_2](CH_3OH) complex recorded in DMF at room temperature consists of a six-line pattern that is typical of monomeric Mn(II) complexes [$g = 2.0011$, $A = 94.14$ G].

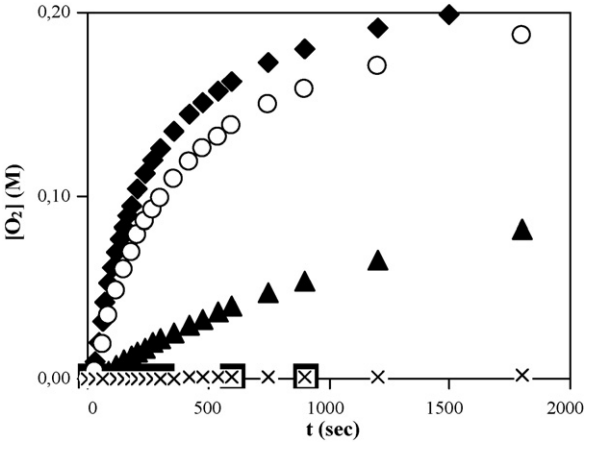

Fig. 2. Disproportionation of H_2O_2: (■) in the presence of [Mn(indH)Cl_2](CH_3OH); (×) in the presence of [Mn(indH)Cl_2](CH_3OH) with 2,6-di-*tert*-butylpyridine; (▲) in the presence of [Mn(indH)Cl_2](CH_3OH) with pyridine (20 equiv.); (◯) in the presence of [Mn(indH)Cl_2](CH_3OH) with imidazole (20 equiv.); (♦) in the presence of [Mn(indH)Cl_2](CH_3OH) with 1-methylimidazole (20 equiv.) at 21 °C. [{Mn^{II}(indH)Cl_2}(CH_3OH)]$_0$ = 2.11×10^{-3} M, [H_2O_2]$_0$ = 4.47×10^{-1} M in 20 cm^3 CH_3CN.

The molecular structure and atom numbering scheme for [Mn(indH)Cl_2](CH_3OH) is shown in Fig. 1, and selected bond lengths and angles are listed in Table 1. The manganese(II) ion has a slightly distorted trigonal–bipyramidal geometry with $\tau = 0.69$ as judged by the method of Addison et al. [25]. Two chloride ions and one nitrogen atom of the isoindoline ligand occupy basal positions. The two other nitrogen atoms of the indH ligand are in apical positions. The Cu–N distance in the basal plane is shorter than those in apical positions.

3.2. Kinetic studies

3.2.1. Catalase-like activity in CH_3CN

The catalase-like activity of the complex [Mn(indH)Cl_2](CH_3OH) to disproportionate H_2O_2 into H_2O and O_2 was examined in CH_3CN at 21 °C by volumetric measurements of evolved dioxygen. The reactivity studies indicated that the complex itself is catalytically almost inactive, but the decomposition of H_2O_2 is enhanced in the presence of a base such as 1-methylimidazole (1-MeimH), imidazole (imH) or pyridine (py) (Fig. 2). Among the various nitrogenous bases investigated in this study imidazole and substituted imidazole with strong π-donating ability show the highest accelerating effect on the disproportionation process. However, 2,6-di-*tert*-butylpyridine had no effect, thus showing that the N-ligands used above were not acting simply as Brønsted bases.

A variation of imidazole concentration revealed saturation behavior supporting the likely coordination of the coligand to the metal center (Fig. 3), so the significant acceleration of the decomposition of H_2O_2 upon addition of pyridine or imidazole reveals a significant push effect. As shown in Fig. 4, linear Hammett correlation with ρ value of −1.63 is obtained for a series of 4′-substituted pyridines, demonstrating that electron-releasing groups enhance the reaction rate. These results may suggest the importance of π-rather than σ-interactions of nitrogenous donors with the metal center. Such a push effect has been prominent in proposed mechanisms for dioxygen activation by heme enzymes (and by their synthetic analog) and emphasizes the role the proximal axial ligand can play in promoting O–O bond cleavage [26,27].

The initial disproportionation rate of H_2O_2 by complex [Mn(indH)Cl_2](CH_3OH) in the presence of excess of imidazole (imH) was measured as a function of the complex and substrate concentrations. At constant [H_2O_2]$_0$, the initial rate of H_2O_2 disproportionation varies linearly with the [catalyst], meaning that the reaction is first-order in catalyst (Fig. 5). The slope of the line gives a first-order rate constant (k) = 0.624 s^{-1}

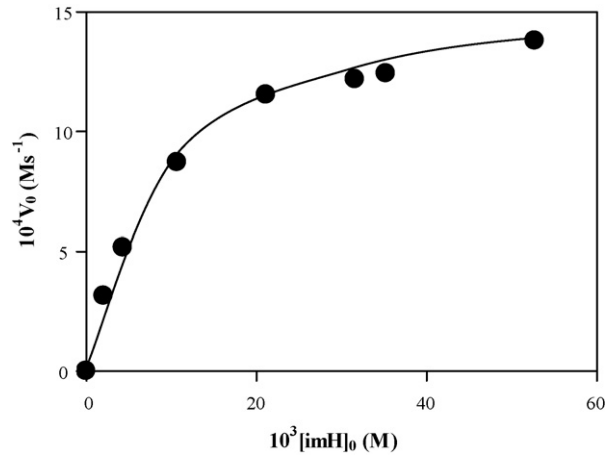

Fig. 3. Dependence of the reaction rate on the imidazole concentration for the [Mn(indH)Cl_2](CH_3OH)-catalyzed disproportionation of H_2O_2. Conditions: [{Mn^{II}(indH)Cl_2}(CH_3OH)]$_0$ = 2.11 × 10^{-3} M, [H_2O_2]$_0$ = 4.47 × 10^{-1} M at 21 °C in 20 cm^3 CH_3CN.

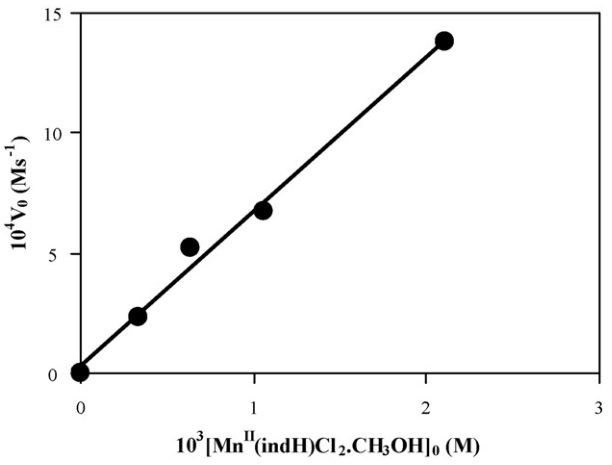

Fig. 5. Dependence of the reaction rates on the [Mn(indH)Cl_2](CH_3OH) concentration for the [Mn(indH)Cl_2](CH_3OH)-catalyzed disproportionation of H_2O_2 in the presence of imidazole. Conditions: [H_2O_2]$_0$ = 4.47 × 10^{-1} M, [imH]$_0$ = 5.28 × 10^{-2} M, at 21 °C in 20 cm^3 CH_3CN.

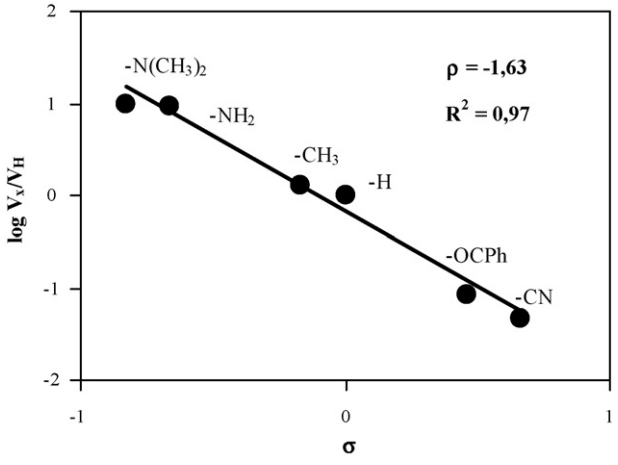

Fig. 4. Plot of log (relative initial rate) vs. σ for the [Mn(indH)Cl_2](CH_3OH)-catalyzed disproportionation of H_2O_2 in the presence of 4R-py. Conditions: [{Mn^{II}(indH)Cl_2}(CH_3OH)]$_0$ = 2.11 × 10^{-3} M, [H_2O_2]$_0$ = 4.47 × 10^{-1} M, [4R-py]$_0$ = 4.22 × 10^{-2} M, at 21 °C in 20 cm^3 CH_3CN.

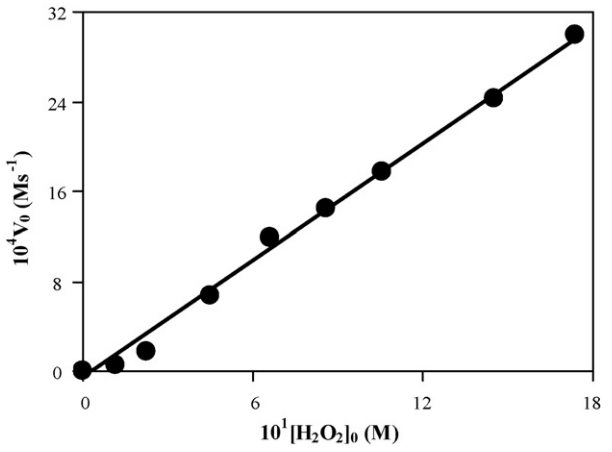

Fig. 6. Dependence of the reaction rate on the H_2O_2 concentration for the Mn^{II}(indH)Cl_2·CH_3OH-catalyzed disproportionation of H_2O_2 in the presence of imidazole. Conditions: [{Mn^{II}(indH)Cl_2}(CH_3OH)]$_0$ = 1.1 × 10^{-3} M, [imH]$_0$ = 5.28 × 10^{-2} M, at 21 °C in 20 cm^3 CH_3CN.

for a H_2O_2 concentration of 447 mM (52.8 mM imH). At low substrate concentrations, the reaction is also first-order in peroxide concentration as shown in Fig. 6, to establish a rate law of-d[H_2O_2]/dt = k_{cat}[H_2O_2][Mn]. The slope of the line provides the bimolecular rate constant for a second-order reaction of 1.55 $M^{-1}s^{-1}$, which is somewhat slower than other published model compounds [28]. The first-order dependence of the reaction rate on the two reactants and the lack of time-lag

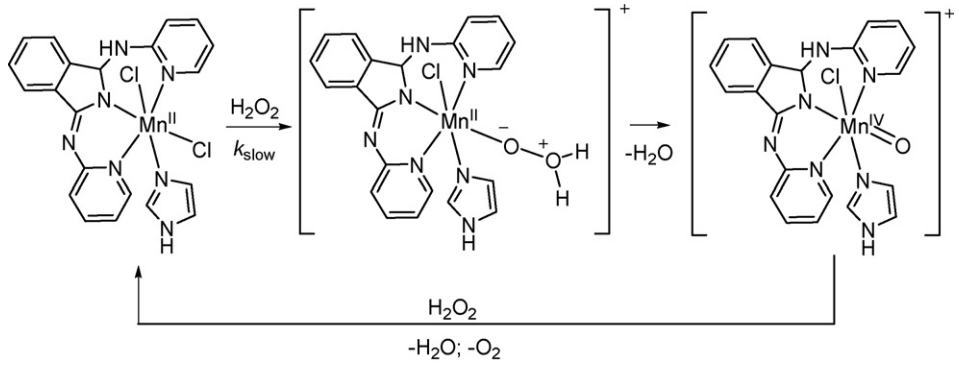

Scheme 1.

at the onset of the reaction suggest that the coligand-containing complexes are responsible for the disproportionation of H_2O_2. Addition of H_2O_2 results in increase of the intensity of the transition at 387 nm, and in a new band at 441 nm (Fig. 7). Similar bands have been assigned to transitions of Mn(IV) complexes [29,30], therefore it may be concluded that metal center of [Mn(indH)(ImH)Cl_2] is transformed from Mn(II) to Mn(IV) on the addition of H_2O_2 (Scheme 1). The same effect could also be observed when instead of H_2O_2 iodosylbenzene was used.

3.2.2. Catalase-like activity in aqueous solution

The catalase-like activity of the complex [Mn(indH)Cl_2](CH_3OH) to disproportionate H_2O_2 into H_2O and O_2 was examined in aqueous solution too. Since the catalytic activity of complex [Mn(indH)Cl_2](CH_3OH) was expected to depend on the pH value of the aqueous solution, the pH dependence of H_2O_2 dismutation was studied between pH 9.16 and pH 10.56. It was found that the initial rate of the disproportionation of H_2O_2 increases with increasing pH and goes through a maximum, which was found at pH ~ 9.6 (Fig. 8). We believe that the activity is influenced by the protonation state of H_2O_2. Assuming that hydrogen peroxide is activated by a direct interaction with the metal center of the complex, decomposition is expected to be favored by a high pH because of the larger concentration of the perhydroxyl anion (HOO^- is more nucleophilic than H_2O_2). On the other hand, at larger pH values, the complexe(s) may be destroyed by the formation of the mineral forms of manganese (Fig. 8).

The kinetic studies on the disproportionation of H_2O_2 were performed in aqueous solution (0.1M carbonate buffer, pH 9.52, $T = 21\,^{\circ}C$) by volumetric measurements of evolved dioxygen. At constant $[H_2O_2]_0$, the initial rate of H_2O_2 disproportionation varies linearly with the catalyst (1:200–1320), meaning that the reaction in aqueous solution is also first-order on $[Mn^{II}(indH)Cl_2{\cdot}CH_3OH]_0$ (Fig. 9). To determine the dependence of the rates on the substrate concentration, solutions of the complex [Mn(indH)Cl_2](CH_3OH) were treated

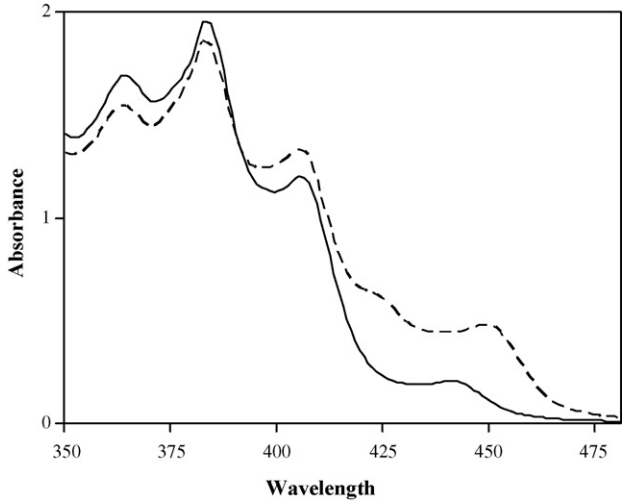

Fig. 7. Absorption of the Mn^{II}(indH)(ImH)Cl_2 solution (in CH_3CN) before (–) and after (—) addition of H_2O_2.

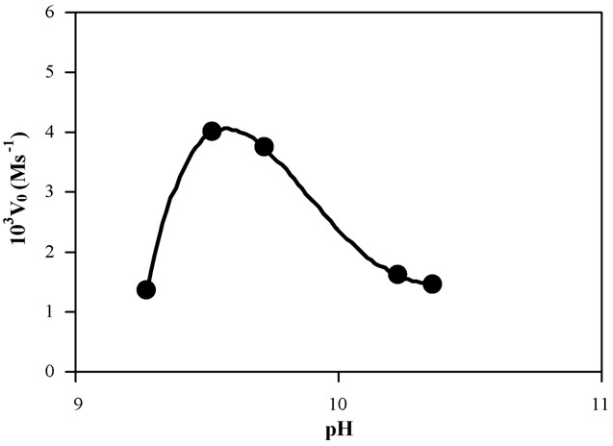

Fig. 8. Dependence of the maximum rate of the [Mn(indH)Cl_2](CH_3OH)-catalyzed disproportionation of H_2O_2. Conditions: [{Mn^{II}(indH)Cl_2}(CH_3OH)]$_0 = 2.11 \times 10^{-4}$ M, $[H_2O_2]_0 = 4.47 \times 10^{-1}$ M at 21 °C in 20 cm^3 aqueous buffer.

with increasing amounts of H_2O_2 (1:500–3600). Under this experimental condition, saturation kinetics was found for the initial rates *versus* the H_2O_2 concentrations. Substrate saturation behavior implies a rapid equilibrium between unbound substrate and a catalyst complex. Under conditions of high substrate concentration, the primary species in solution is the catalyst–substrate complex. The rate of the reaction is dependent only on the decomposition of the catalyst–substrate complex (r.d.s.) to the product and the free catalyst. An analysis of the data based on the Michaelis–Menten model, originally developed for enzyme kinetics, was applied. The results evaluated from Lineweaver–Burk plots (Fig. 10) are $V_{max} = 8.1 \times 10^{-3}\,Ms^{-1}$, $K_M = 489$ mM, $k_{cat} = 38 \pm 2\,s^{-1}$ and $k_2(k_{cat}/K_M) = 79 \pm 4\,M^{-1}s^{-1}$. The data presented illustrate that the catalyst has relatively high turnover number (k_{cat}) but appears to bind peroxide very badly. Since K_M is related to the formation of the catalyst–substrate complex, its relatively high value is consistent with a proton-dependent step being involved with substrate binding. The catalytic activity

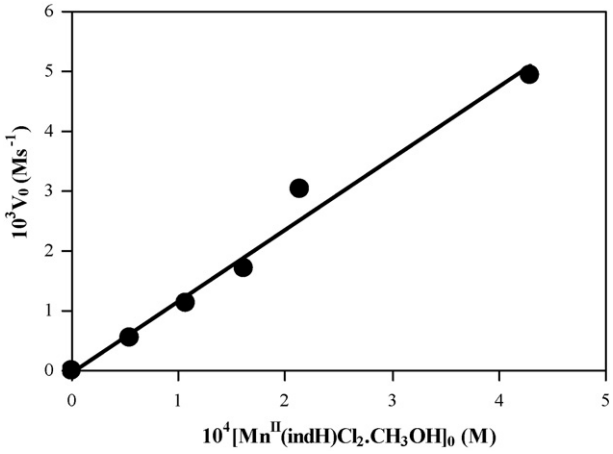

Fig. 9. Dependence of the reaction rates on the [Mn(indH)Cl_2](CH_3OH) concentration for the [Mn(indH)Cl_2](CH_3OH)-catalyzed disproportionation of H_2O_2 Conditions: $[H_2O_2]_0 = 2.84 \times 10^{-1}$ M, at 21 °C in 20 cm^3 aqueous ammonium hydroxide buffer.

Table 3
Kinetic parameters of reported H_2O_2 disproportionation catalysts

Catalyst	k_{cat} (s^{-1})	K_M (mM)	k_{cat}/K_M ($s^{-1}M^{-1}$)	Ref.
Thermus thermophilus	2.6×10^5	83	3.1×10^6	[35]
Lactobacillus plantarum	2.0×10^5	350	0.6×10^6	[36]
Thermoleophilium album	2.6×10^4	15	1.7×10^6	[6]
$[Mn(bpia)(\mu\text{-}OAc)]_2(ClO_4)_2$[a]	1.1×10^3	31.5	3.4×10^4	[33]
$[Mn(salpn)O]_2$[b]	2.5×10^2	250	1.0×10^3	[28,32]
$Mn^{II}(indH)Cl_2$	38.9	489	79.2	This work
$[Mn(2\text{-}OH(Xsal)pn)]_2$[c]	4.2–21.9	10.2–118	160–990	[28,34]
$[Mn(ind)_2]$	6.0×10^{-2}	19	3.2	[23]
$[Mn(H_2O)_6](ClO_4)_2$	6.3×10^{-3}	–	–	[28]

[a] bpa: bis(2-picolyl)(*N*-methylimidazole-2-yl)-amine.
[b] H_2salpn: *N*,*N*′-bis(salicylidene)-1,3-diaminopropane.
[c] H_3(2OHsalpn: *N*,*N*′-bis(salicylidene)-2-hydroxy-1,3-diaminopropane.

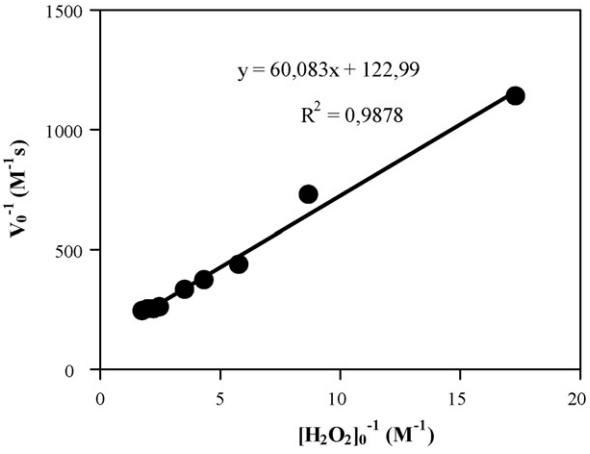

Fig. 10. Lineweaver–Burk plots for the $[Mn(indH)Cl_2](CH_3OH)$-catalyzed disproportionation of H_2O_2 Conditions: $[\{Mn^{II}(indH)Cl_2\}(CH_3OH)]_0 = 2.11 \times 10^{-4}$ M, at 21 °C in 20 cm^3 aqueous ammonium hydroxide buffer (pH 9.52).

shown by $[Mn(indH)Cl_2](CH_3OH)$ is similar to that of two classes of dimanganase complexes with $(\mu\text{-alkoxo})_2Mn_2$ and $(\mu\text{-alkoxo})(\mu\text{-acetato})Mn_2$ cores, which also catalyses H_2O_2 dismutation with saturation kinetics and similar k_{cat}, but with lower rate than those found of $[Mn(bpia)(\mu\text{-}OAc)]_2(ClO_4)_2$ and $[Mn(salpn)O]_2$ complexes (Table 3) [31–34].

4. Conclusion

This study has demonstrated that the complex $[Mn(indH)Cl_2](CH_3OH)$ in the presence of a base such as 1-methylimidazole, imidazole or pyridine is an efficient catalyst for the disproportionation of H_2O_2 in CH_3CN. Among the various nitrogenous bases investigated in this study imidazole and substituted imidazole with strong π-donating ability show better co-catalytic effect, thus providing nucleophilic assistance to the rate-determining step.

In case of aqueous solution the complex $[Mn(indH)Cl_2](CH_3OH)$ shows much higher catalytic activity, and the initial rate of the disproportionation of H_2O_2 increases with increasing pH and goes through a maximum, which was found at pH ∼ 9.6. In this pH value the reaction shows first-order dependence on the catalyst, and saturation kinetics on $[H_2O_2]$.

These data suggest that the catalytic activity of the indH–Mn(II) complex depends not only on the electronic properties of the complex modulated by the π-donating coligands but also on secondary effects including the solvent, the thermodynamic complex stability and the pH of the solution. Further work is in progress on other manganese-containing functional catalase models.

Acknowledgments

Financial support of the Hungarian National Research Fund (OTKA K67871), COST, Budaconsum Ltd., and Ulrich Trade Ltd. is gratefully acknowledged.

Appendix A. Supplementary data

Supplementary data associated with this article can be found, in the online version, at doi:10.1016/j.molcata.2007.11.005.

References

[1] R.S. Balaban, S. Nemoto, T. Finkel, Cell 120 (2005) 483.
[2] F.J. Giordano, J. Clin. Invest. 115 (2005) 500.
[3] Y. Kono, I. Fridovich, J. Biol. Chem. 258 (1983) 6015.
[4] Y. Kono, J. Biol. Chem. 258 (1983) 13646.
[5] V.V. Barynin, A.I. Grebenko, Dokl. Akad. Nauk SSSR 286 (1986) 461.
[6] G.S. Algood, J.J. Perry, J. Bacteriol. 168 (1986) 563.
[7] J. Mizobata, M. Kagawa, N. Murakoshi, E. Kusaka, K. Kameo, Y. Kawata, J. Nagai, Eur. J. Biochem. 267 (2000) 4264.
[8] T. Amo, H. Atomi, T. Imanaka, J. Bacteriol. 184 (2002) 3305.
[9] V.L. Kinnula, J.D. Crapo, Am. J. Respir. Crit. Care Med. 167 (2003) 1600.
[10] D.P. Riley, Chem. Rev. 99 (1999) 2573.
[11] B.J. Day, Drug Discov. Today 9 (2004) 557.
[12] S.R. Doctrow, K. Huffman, C.B. Marcus, G. Tocco, E. Malfroy, C.A. Adinolfi, H. Kruk, K. Baker, N. Lazarowych, J. Mascarenhas, B. Malfroy, J. Med. Chem. 45 (2002) 4549.
[13] Y. Watanabe, A. Namba, N. Umezawa, M. Kawahata, K. Yamaguchi, T. Higuchi, Chem. Commun. (2006) 4958.
[14] R.R. Gagné, D.N. Marks, Inorg. Chem. 23 (1984) 65.
[15] C.A. Tolman, J.D. Druliner, P.J. Krusic, M.J. Nappa, W.C. Seidel, I.D. Williams, S.D. Ittel, J. Mol. Catal. 48 (1988) 129.
[16] É. Balogh-Hergovich, J. Kaizer, G. Speier, G. Huttner, A. Jacobi, Inorg. Chem. 39 (2000) 4224.
[17] É. Balogh-Hergovich, G. Speier, J. Mol. Catal. A: Chem. 230 (2005) 79.
[18] D.F. Shriver, M.A. Drezdzon, The Manipulation of Air-sensitive Compounds, John Wiley & Sons, New York, 1986.

[19] D.D. Perrin, W.L. Armarego, D.R. Perrin, Purification of Laboratory Chemicals, 2nd ed., Pergamon, New York, 1990.
[20] W.O. Siegl, J. Org. Chem. 42 (1977) 1872.
[21] G.M. Sheldrick, SHELXL97. Program for the Refinement of Crystal Structures, University of Göttingen, Germany, 1997.
[22] J. Kaizer, J. Pap, G. Speier, M. Réglier, M. Giorgi, Transit. Met. Chem. 29 (2004) 630.
[23] J. Kaizer, G. Baráth, G. Speier, M. Réglier, M. Giorgi, Inorg. Chem. Commun. 10 (2007) 292.
[24] R.J. Letcher, W. Zhang, C. Bensimon, R.J. Crutchley, Inorg. Chim. Acta 210 (1993) 183.
[25] A.W. Addison, T.N. Rao, J. Reedijk, J. van Rijn, G.C. Verschoor, J. Chem. Soc., Dalton Trans. (1984) 1349.
[26] M. Sono, M.P. Roach, E.D. Coulter, J.H. Dawson, Chem. Rev. 96 (1996) 2841.
[27] J. Kaizer, M. Costas, L. Que Jr., Angew. Chem. Int. Ed. 42 (2003) 3671.
[28] A. Gelasco, S. Bensiek, V.L. Pecoraro, Inorg. Chem. 37 (1998) 3301.
[29] D.E. De Vos, T. Bein, J. Organomet. Chem 520 (1996) 195.
[30] A.A. Belal, P. Chaudhuri, I. Fallis, L.J. Farrugia, R. Hartung, N.M. McDonald, B. Nuber, R.D. Peacock, J. Weiss, K. Wieghardt, Inorg. Chem. 30 (1991) 4397.
[31] A.C. Rosenzweig, C.A. Frederick, S.J. Lippard, P. Nordlund, Nature 366 (1993) 537.
[32] E.J. Larson, V.L. Pecoraro, J. Am. Chem. Soc. 113 (1991) 7809.
[33] M.U. Triller, W.Y. Hsieh, V.L. Pecoraro, A. Rompel, B. Krebs, Inorg. Chem. 41 (2002) 5544.
[34] A. Galesco, V.L. Pecoraro, J. Am. Chem. Soc. 115 (1993) 7928.
[35] M. Shank, V. Barynin, G.C. Dismukes, Biochemistry 33 (1994) 15433.
[36] J. Penner-Hahn, in: V.L. Pecoraro (Ed.), Manganese Redox Enzymes, VCH Publishers, New York, 1992, p. 29.